Science and Technology for the Built Environment, (2022) **0**, 1–17

ISSN: 2374-4731 print / 2374-474X online
DOI: 10.1080/23744731.2022.2127621

The borehole thermal energy storage at Emmaboda, Sweden: First distributed temperature measurements

RANDI K. RAMSTAD[1,2]*, MARIA JUSTO ALONSO[3], JOSÉ ACUÑA[1,4], OLOF ANDERSSON[5], MILAN STOKUCA[4], NIKLAS HÅKANSSON[6], KIRSTI MIDTTØMME[7] and LEIF RYDELL[6,8]

[1]*Department of Geoscience and Petroleum, Norwegian University of Science and Technology, Trondheim, Norway*
[2]*Asplan Viak AS, Trondheim, Norway*
[3]*SINTEF Community, Trondheim, Norway*
[4]*Bengt Dahlgren AB, Stockholm, Sweden*
[5]*Geostrata HB, Södra Sandby, Sweden*
[6]*Xylem Water Solutions Manufacturing AB, Emmaboda, Sweden*
[7]*NORCE Norwegian Research Centre AS, Bergen, Norway*
[8]*Reikab AB, Emmaboda, Sweden*

Xylem in Emmaboda, Sweden, has one of the first borehole thermal energy storage (BTES) sites storing excess heat and has been previously thoroughly studied and monitored. Here, the results from distributed temperature sensing (DTS) measurements in observation boreholes, UB1, 10 m outside the BTES, and UB46, inside the BTES, are presented. The measurements were performed in February and March to September 2019. DTS combined with geological and hydrogeological knowledge give qualitative insights into Emmaboda's heat transfer in operation. To analyze the DTS measurements, knowledge about the borehole deviations and relative physical locations among boreholes is necessary. The measured temperature profile in UB1 is parallel to the geothermal gradient, follows BTES temperature, and does not seem disturbed by groundwater flow and production boreholes. The flat terrain and several rivers and dams in the area, together with results from the thermal response test following the mineralogical composition of the bedrock, verify no regional groundwater flow. Emmaboda's heat loss is conductive only. In UB46, the temperature irregularities are interpreted as contact points or vicinity to production boreholes. Larger temperature responses in heat charging than in extraction mode are probably due to higher temperatures. Three-dimensional to four-dimensional design, documentation and visualization should further examine the influence of borehole deviation.

Introduction

Space heating and domestic hot water needs may represent 54% (Statens energimyndighet 2020) and up to 60% (Justo-Alonso and Stene 2013) of the total energy demand of the building sector in cold areas. By 2008 in Norway, up to 19 TWh of industrial waste heat was used for heating purposes (Sevault, Stavset, and Bantle 2017). Excess heat from industrial processes is estimated to be 812 TWh/year in Europe (EU27) (Persson, Moller, and Werner 2014). However, much of this heat is not used due to a low match between demand and availability. For instance, household waste cannot be stored to be burned only in the winter, and excess heat during summer cannot be used for direct heating and should be saved as a heat source for energy storage.

A borehole thermal energy storage (BTES) consists of several densely packed closed-loop borehole heat exchangers (BHEs) employed to create sensible heat storage underground. Increased use of heat recovery and heat storage would increase one of the main bottlenecks of district heating for the usage of this surplus heat (Brange et al. 2017). Using energy from waste burning could provide heat at 85 °C, which enables storage temperatures in a BTES at 45–60 °C (Jokiel et al. 2020). This storage temperature connected to a heat pump can supply

Received March 4, 2022; accepted September 13, 2022
Randi Kalskin Ramstad, Dr.ing., is an Associate Professor II and Consultant. **Maria Justo Alonso, M.Sc.,** is a Researcher and PhD-student. **José Acuña, PhD,** is the CEO of Bengt Dahlgren Stockholm Geo AB. **Olof Andersson, PhD,** is a Senior Researcher and Consultant. **Milan Stokuca, Civ.ing,** is a Consultant. **Niklas Håkansson, Ing.,** is an Energy and Production Engineer. **Kirsti Midttømme, Dr.ing.,** is a Chief Scientists. **Leif Rydell, Ing.,** is a Consultant.
*Corresponding author e-mail: Randi.kalskin.ramstad@ntnu.no; RandiK.Ramstad@asplanviak.no

Table 1. Summary of other existing HT-BTES, their heat source, and the maximum storage temperature.

High-temperature BTES	Heat source	Maximum temperature (°C)	Designed use of the heat stored
Anneberg, Solna, SE (Regander 2019)	Solar thermal	55	Space heating
Attenkirschen, Germany (Regander 2019)	Solar thermal	50	District heating (via heat pump) and space heating
Braedstrup, Danmark (Røgen et al. 2015)	Solar thermal	60	District heating (via heat pump)
Crailsheim, Germany (Schneider 2013)	Solar thermal	65	District heating (via heat pump)
Necklarsum, Germany (Nußbicker et al. 2003)	Solar thermal	65	District heating with auxiliary boiler
Oktokos, Canada (Rad, Fung, and Rosen 2017)	Solar thermal	74	Space heating
Paskov, Czech Republic (Klempa et al. 2014)	Combined heat and power	95	Experimental: rock behavior in different charging–discharging
GeoTermos, Norway (Justo-Alonso et al. 2020).	Outdoor air + solar thermal (photovoltaic-driven CO_2 heat pump)	60–65	Space heating

temperatures to district heating at more than 70 °C or direct supply domestic hot water and space heating of building complexes. Storage sites are also well suited for harvesting renewable energy sources (Winterscheida, Dalenbäcka, and Hollerb 2017). A BTES stores the heat produced when it is accessible and uses it when needed, contributing to more continuous and optimum operation of the machinery (Lanahan and Tabares-Velasco 2017).

The availability of many renewable energy sources fluctuates widely and does not always match demand profiles (Sibbitt et al. 2012). BTES systems could be seen as part of the solution to cope with the seasonal mismatch. Drake Landing is a demonstration site in Canada finalized in 2007, and has been operating since with a BTES core temperature between approximately 40 and 65 °C to cover space heating only at a maximum temperature of 55 °C (Reuss and LFBT-A in TESS 2021). This project demonstrates the feasibility of using BTES to store solar energy (Mesquita et al. 2017). Fjell 2020 is a school where a similar concept (GeoTermos) is demonstrated in Drammen, Norway (Ramstad et al. 2017). Here, the heat stored in the BTES from 2020 is obtained from outdoors air via a CO_2 heat pump and solar energy. The storage temperature is 50–55 °C during charging to supply directly low-temperature space heating at 25 °C (Justo-Alonso et al. 2020). However, for periods of high heating demands, it is possible to use the BTES as the heat source for the heat pump, as was necessary in winter 2021/2022. Table 1 summarizes other existing high-temperature BTES. High-temperature BTES (HT-BTES) temperature ranges from ∼25 °C to ∼90 °C (Kallesøe and Vangkilde-Pedersen 2019). In Necklarsum, heat pumps are used for heat extraction, while at Anneberg, direct heat exchange is used (Nilsson 2020). In Emmaboda, Sweden, industrial waste heat is used as the heat source for the BTES. Some of these storages did not attain the design storage temperature due to too small solar collectors or changes in the operation strategies. More information about these BTES sites can also be found in Malmberg (2017).

Good control of a BTES is recommended to increase its profitability (Andersson, Håkansson, and Rydell 2021a), given that the technology is relatively new (Skarphagen et al. 2019). The performance of BTES systems depends on the temperatures circulated in the boreholes and the distribution system using the stored heat. Having a single measurement at the common point from/to the BTES, meaning a reduced level of detail, is state of the art. In order to get a more realistic picture of the processes happening in the BTES and on single boreholes, distributed temperature sensing (DTS) is a powerful tool in supporting heat transport understanding. DTS can be used to characterize and understand thermal dynamics, but also heat tracer tests with DTS can be used to estimate evaporation (Schilperoort et al. 2018), groundwater–surface water interaction (Lowry et al. 2007), groundwater flow (Bakker et al. 2015; Bense et al. 2016), fractures, and underground heat distribution (Kvalsvik et al. 2022).

DTS measurements for monitoring BTES are becoming more widespread. The Akademiska hus (Tjernstrom et al. 2016), the Stockholm University Campus (Monzo, Lazzarotto, and Acuna 2017), Fjell skole (Ramstad et al. 2017), and Braedstrup (Malmberg et al. 2018) have DTS installed to increase knowledge of the BTES.

Objective

As one of the first HT-BTES sites in the world, the Emmaboda site has been thoroughly studied and documented. Extensive knowledge of the system, including characteristics of the geology, hydrogeology, and drilling aspects such as borehole deviation, penetration rate, and water-bearing fracture zones, is available.

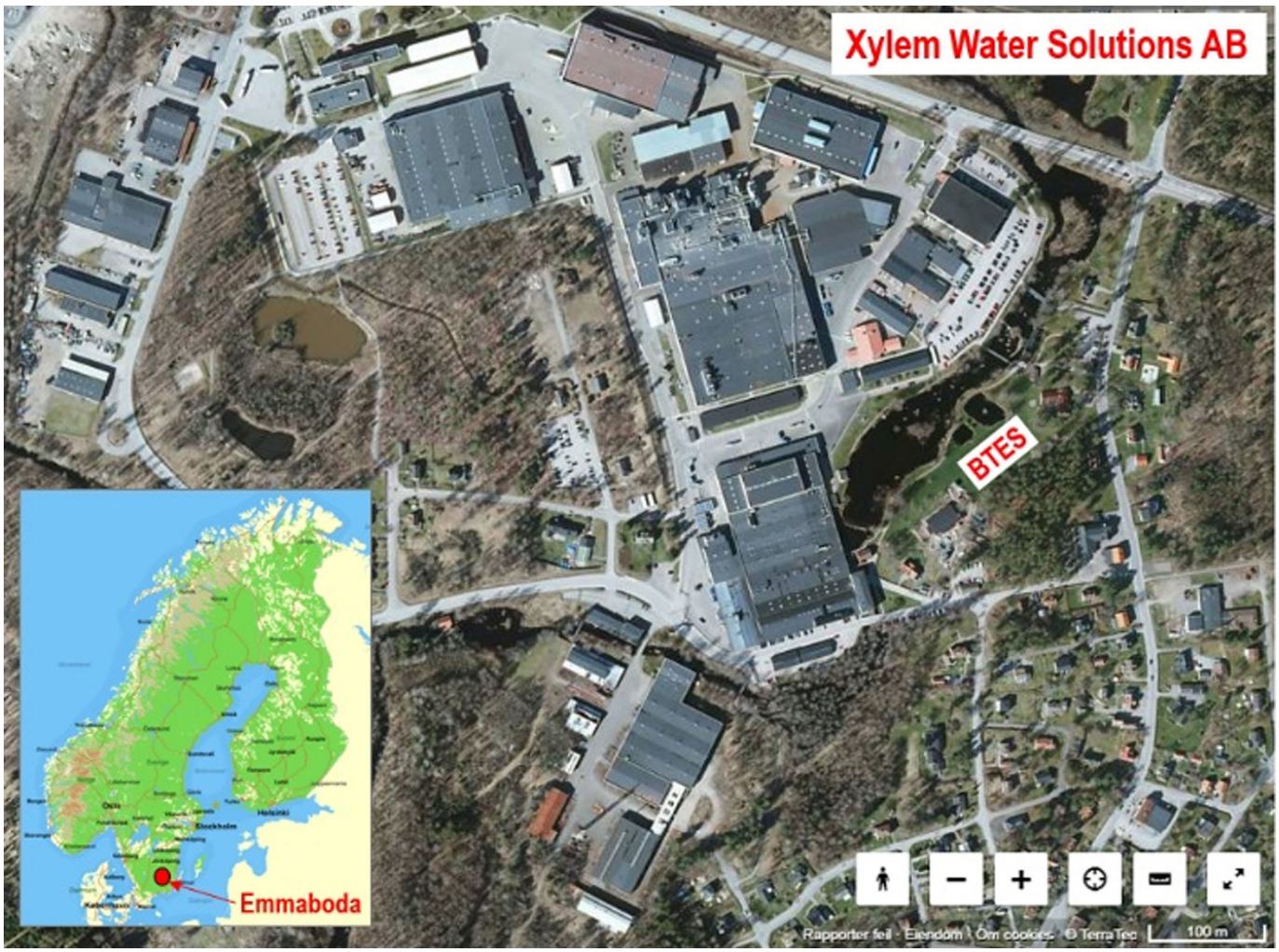

Fig. 1. The location of the BTES at the Xylem manufacturing plant at Emmaboda (map from www.gulesider.no).

The purpose of the DTS measurements at the Emmaboda site is to build further on this existing and extensive knowledge for a BTES in operation. The DTS in this work is used to verify and give additional information, and better insights and understanding of the BTES behavior are achieved. This knowledge is essential for the further development of the HT-BTES technology in terms of short-term and long-term performances and flexible operation.

Therefore, the main objective of this work is to increase understanding of the heat transfer and the specific on-site geological conditions in the HT-BTES at Xylem, Emmaboda, using distributed temperature measurements under normal operating conditions:

- Study the relationship between the temperature profiles, hydrogeology and borehole deviation.
- Study the temperature response of the storage to heat extraction and heat charging.
- Visualize the temperature profiles inside and nearby the HT-BTES during operation.

To the authors' knowledge, most of the available research focuses on operational measurements at research sites. Knowledge and understanding of the performance of sites under real conditions are lacking and are needed to improve design and operation. Thus, this article analyzes the measurements at the Emmaboda site after several years of operation, also deploying DTS measurements that give a more insightful detail to the BTES performance. Hopefully, the Emmaboda results will be helpful for the further development of this technology that allows storing heat from summer to winter in the energy transition.

Methods

Site description

The BTES at Xylem Water Solutions AB, Emmaboda, is in the southeastern part of Sweden (Figure 1). Several publications (i.e., Andersson, Rydell, and Algotsoon 2009; Nordell et al. 2014, 2016), describe the planning, installation, operation, and experiences of the BTES thoroughly. The modification from direct use of the storage heat to the installation of a heat pump system is described in Rydell (2019). The BTES has been in operation since 2010, storing the excess heat from the manufacturing of Xylem pumps.

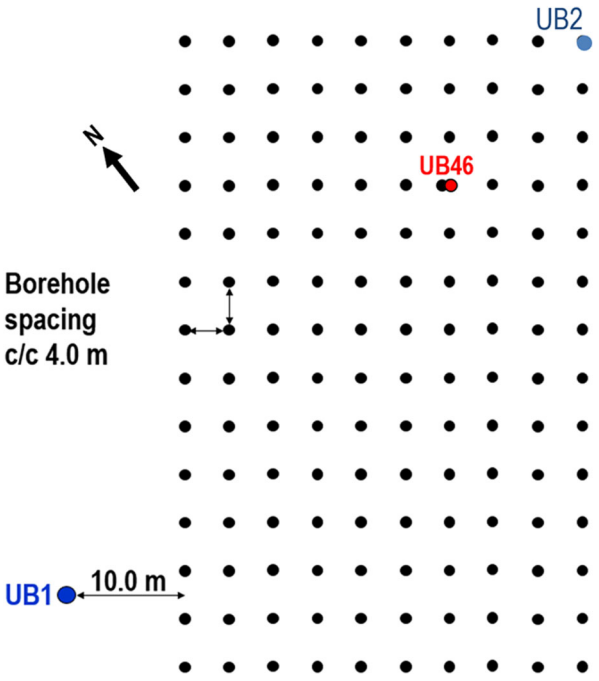

Fig. 2. The BTES at Emmaboda consists of 140 boreholes, each with a depth of 150 m and 4 m of spacing. The observation boreholes UB1 and UB46 are located outside and inside the BTES. UB2 is the borehole in the upper right corner. Modified after Nordell et al. (2014).

The BTES consists of 140 boreholes with a borehole depth of 150 m (Figure 2). The temperatures inside and outside the storage have been measured by PT100 sensors placed in the observation boreholes UB1 and UB46 located outside and inside the storage, respectively (see Figures 2–5). These two boreholes have been further equipped with optical fiber cables for distributed temperature measurements. A picture from the installation work is shown in Figure 6.

The surface of the BTES is insulated with 40 cm of foam glass, which consists of expanded recycled glass with thermal conductivity of 0.13–0.15 W/mK (Nordell et al. 2016). The picture in Figure 6 from installing the fiber cable and the snow-covered surface shows that the surface insulation works as intended. The temperature in the bedrock at the time was around 30–35 °C.

Hydrogeological and geological conditions

The hydrogeological and geological conditions of the Emmaboda BTES are described in detail by Nordell et al. (2016). The bedrock consists of granodiorite. Three thermal response tests were performed in the area, resulting in an average effective thermal conductivity value of 3.0 W/m·K (two old tests with 2.8 and 3.2 on the other side of the dam and 3.0 W/m·K in UB2).

A large fracture zone at the western border of the storage (Figure 7) intersects the observation borehole UB1 at 30 m. The area is flat, and the groundwater level is stable throughout the year, being controlled by the pond connected to several others rivers and dams (Figures 1 and 7). Borehole drilling revealed that the bedrock has several water-filled fractures and unstable cross-zones and therefore has a fracture permeability. Around 30% of the boreholes had an air-lift or groundwater capacity of more than 500 L/min (Nordell et al. 2016).

While drilling a borehole, the direction of the drill may change (Moldashi 2021). The deviation may be due to heterogeneous formations, unequal pressure applied during drilling, weight on the bit, hydraulics in the site, or many other reasons (Murphey and Cheatham 1966). In Emmaboda, the boreholes were drilled with two-point steering control. In theory, they are expected to be vertical. Twenty-one randomly selected boreholes were measured by a gyro inclinometer (Nordell et al. 2016) to draw correct inference from borehole deviations. The results presented in Figure 8 (Nordell et al. 2016) show that nine boreholes deviated toward the northwest and five toward the northeast. Some boreholes deviated southwest in the southwestern part of the storage. The deviation varied between 4 and 26 m, with an average deviation of 16 m. The borehole deviation was evaluated to be acceptable concerning the thermal performance of the BTES since most of the boreholes were leaning in the same direction or groups of directions (Nordell et al. 2016). It was concluded that the most reasonable reason for the deviations is the rock structure.

Borehole 46 was selected as an observation borehole (UB46) since it could not be used as a production borehole, as it was drilled into borehole 21 in its deviation toward the south. The assumed borehole path for UB46 is shown in Figure 9 and is close to borehole 34. The measured deviation for boreholes 31 and 33 shows that these boreholes can be quite near UB46 (Figures 8 and 9). The soil cover and casing depth in UB46 are 5 and 9 m below the surface, respectively. A new production borehole 46 was drilled, which explains why two holes with the same number are illustrated in Figure 9.

Fluid flow in the borehole heat exchanger (BHE) for heat extraction and charging

The BHE at Emmaboda is an open coaxial (pipe-in-pipe) system with a central pipe made of polypropylene, with a maximum long-term operation temperature of 65–70 °C. The collector fluid or heat carrier is water.

During heat discharging, the water circulates through the borehole in direct contact with the borehole wall, which can be considered the "outer pipe" in the coaxial collector and returns in the internal coaxial pipe, as shown in Figure 10. Some of the circulated water will leak into permeable fracture zones in the borehole wall. In heat charging mode, water is injected inside the central pipe and reversed for heat extraction (in discharging mode); see Figure 10 (Nordell et al. 2014) or see Morchio, Fossa, and Beier (2022) for further explanations about the flow in coaxial collectors. The general advantage of a coaxial pipe-in-pipe system is the low thermal resistance ensuring an effective heat exchange between the bedrock and the heat carrier. Low pressure losses are also an advantage (Holmberg et al. 2016; Acuña 2013). Unfortunately, the commercial development of coaxial collectors has been slow. Experiences from the two 800-m-deep boreholes in Asker, Norway, showed that developing cost-effective coaxial collectors with high hydraulic

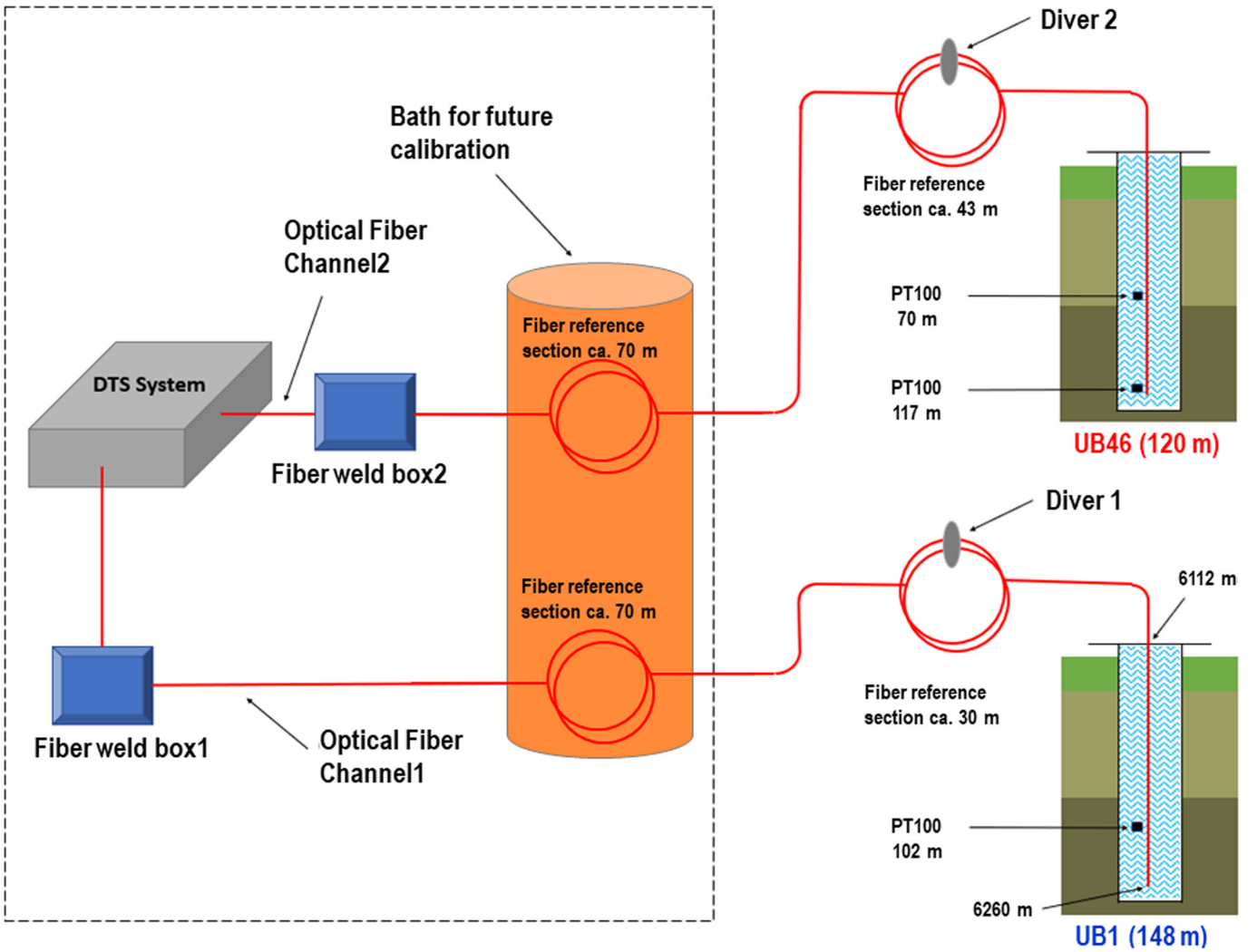

Fig. 3. Installation of fiber optic cable and the DTS system (Stokuca and Acuña 2019). A Mini Diver for temperature calibration is installed at the boreholes and in the technical room. The PT100 temperature sensors in the boreholes have measured the storage temperature since 2010 (Stokuca and Acuña 2019).

and thermal performance that is easy to install is challenging (Ramstad et al. 2020).

The temperature monitoring of the heat carrier (circulating water entering and leaving the BTES) is done using two temperature sensors, GT1a and GT2a. These show the supply or return flow, depending on whether the borehole is in heat charging or heat extraction mode (Figure 11). Note that the flow direction is reversed, meaning that the supply and return temperature of GT1a or GT2a are switched as well.

DTS measurements

Fiber optical cables were installed in the observation boreholes on February 7, 2019 (Figures 6 and 9). The existing PT100 sensors were temporarily removed for the fiber installation and then placed back again at the initial depth. Figure 3 shows a sketch of the main parts of the fiber installation and the DTS system. A Mini Diver for temperature calibration was installed at the boreholes and in the technical room. The fiber optical cable is of type BRUsens Temperature 85 °C and is led into the "technical room" close to the storage (see Figure 3 for details). The fiber was connected to an Oryx datalogger.

The datalogger automatically calibrates the DTS data using an internal mechanism to eliminate the attenuation effect. Typically, the longitudinal attenuation is corrected by introducing an expected differential loss of power along the optical fiber to the DTS system (Ghafoori, Vidmar, and Kryžanowski 2022). Internal calibration can be improved by assigning a reference section or point with a known temperature along the fiber and placing the precise thermometer (e.g., PT100) attached to the DTS system (Ghafoori, Vidmar, and Kryžanowski 2022).

Calibration of the DTS was performed only for UB1, as the data from the divers located in UB46 could not be retrieved. According to the manufacturer (Sensornet 2018), the logger has an accuracy of ±0.5 °C that can be improved by on-site calibration. A mean offset of ∼0.7 K and a standard deviation of about 0.036 K were calculated by analyzing the data for UB1. This error is in line with other results obtained with the same equipment presented in Kvalsvik et al. (2022). This error was deemed satisfactory

Fig. 4. Installation of optical fiber cable in the observation borehole UB1 outside the BTES.

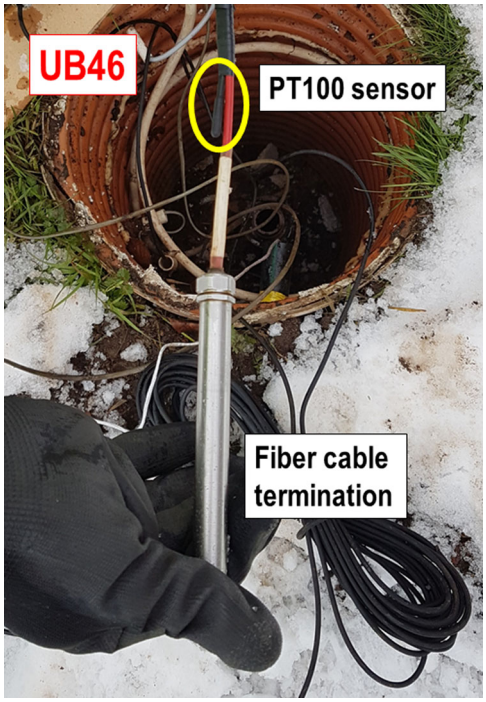

Fig. 5. Fiber cable (red) termination in observation borehole UB46 inside the BTES. The PT100 sensor is placed (black cable) just above the termination.

to give insight into temperature variation and distribution (Kvalsvik et al. 2022), and the same reasoning was applied in this work. Additionally, for this work, the aim of the analysis is the temperature variation and trends to understand the dynamics of BTES in operation to develop future BTES.

The temperature profile was measured every fifth minute and for every half a meter from March 19 to September 5. Since the boreholes are open, the fiber cables measured the temperature of the groundwater inside the boreholes. The fiber cables are expected to lie randomly from the borehole's middle to the borehole's wall. More details of the installation in UB1 and UB46 are seen in Figures 4 and 5, respectively.

In addition to the fiber measuring equipment, the site is monitored in detail via an industrial energy management system. The supply and return temperatures (GT1a and GT2a) to the BTES, the energy supplied and extracted to the BTES, the water flow rate, and the pressure drop in the heat exchangers are measured every 10 min. For the analysis in the present article, temperatures and heat extracted and charged are used to analyze the inertia and sensitivity of the BTES to heat exchange.

Besides DTS measurements, energy extraction and charging magnitudes were obtained to analyze the actual borehole capacity concerning the observed temperatures in the observation boreholes UB1 and UB46.

Results and discussion

Note that the location and the three-dimensional (3D) deviation of the borehole paths presented in Figure 9 are vital to analyzing and understanding the temperature developments in UB46.

Initial operation results from Emmaboda

The modified system using heat pumps to upgrade the supply temperature started operation on September 1, 2018. The heat extraction and charging of the storage followed the regular operation of the factory. The excess heat used for charging was around 55–60 °C. The bedrock temperature had steadily increased to 40–45 °C from 2010 to 2018. This temperature decreased with the heat extraction from late 2018, as Figure 12 shows. Figure 12 is connected to the operation of the BTES:

- There was primarily heat injection during the first years (2011–2013).
- From 2014 to 2017 there was heat charging and some heat extraction. Due to the nature of the coaxial flow during heat extraction (Figure 10), the temperature is higher in the deepest part of the borehole. The change in the ground conductivity based on the flow direction based on the flow in the annular pipe or the central pipe is also discussed in Morchio and Fossa (2020) with similar conclusions.
- From the end of 2017 until September 2018, the system had minimal operation until the beginning of the heat pumps for heat extraction (September 2018). The significantly higher temperature in the middle part of the BTES (at 70 m depth in UB46) compared with the deeper temperature at 117 m depth might be explained by the BTES's minimal operation. The temperature at 117 m might be more exposed for heat loss to the undisturbed temperature below the BTES.

Fig. 6. Installation of fiber cable in observation borehole UB46 inside the BTES and location of UB1 outside the storage. Both fiber cables are lead through cable pipes and connected to the DTS system in the technical room.

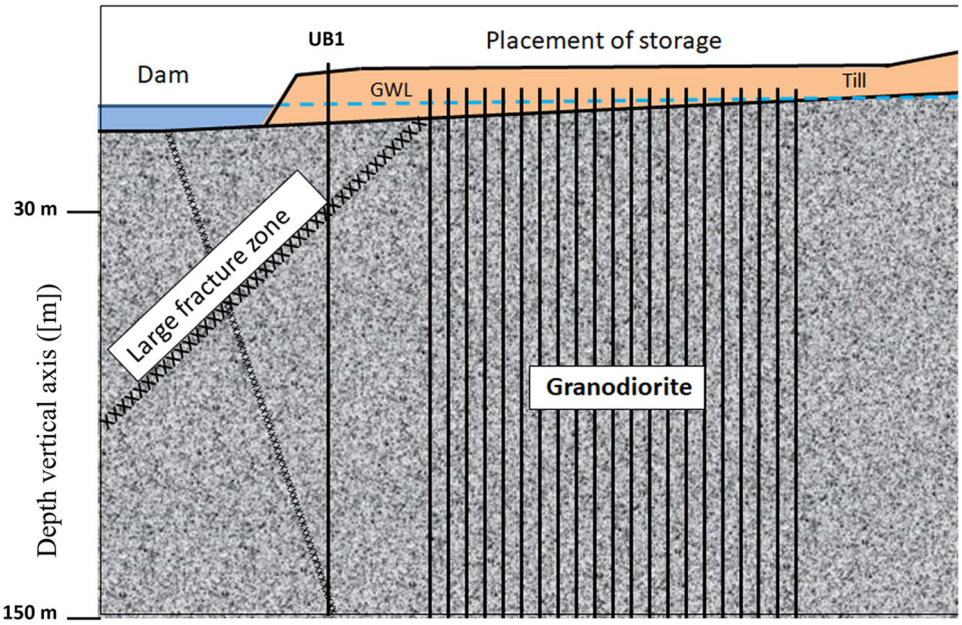

Fig. 7. Hydrogeological and geological conditions in the east–west cross section of the BTES. The large fracture zone in the west is present at 30 m depth in UB1 (western borehole shown on the left-hand side). The 30 m point is illustrated where the black x-line crosses the solid black UB1 line. The bedrock consists of granodiorite. The orange color in the upper part of the figure shows the thickness of the overburdened till. The dam controls the groundwater level (blue dotted line).

- In periods of high heat extraction, for example, January–February 2019 and 2020, the temperature in the storage measured at 117 m depth in UB46 drops below the temperature in the surroundings measured in UB1. Mixing effects might also justify that the temperature at 117 m is lower than at 70 m in UB46.

The temperature development in Figure 12 is affected by the borehole deviation, as explained in Figures 8 and 9. Additionally, Morchio et al. (2020) argue that the direction of the carrier fluid in a coaxial borehole affects the thermal conductivity. Such an effect should be further analyzed concerning heat transfer rates during operation.

Initial analysis of temperature profiles related to hydrogeology and borehole deviation

Figure 13 shows the results from the first DTS temperature profiles measured in UB1 and UB46 on February 7, 2019.

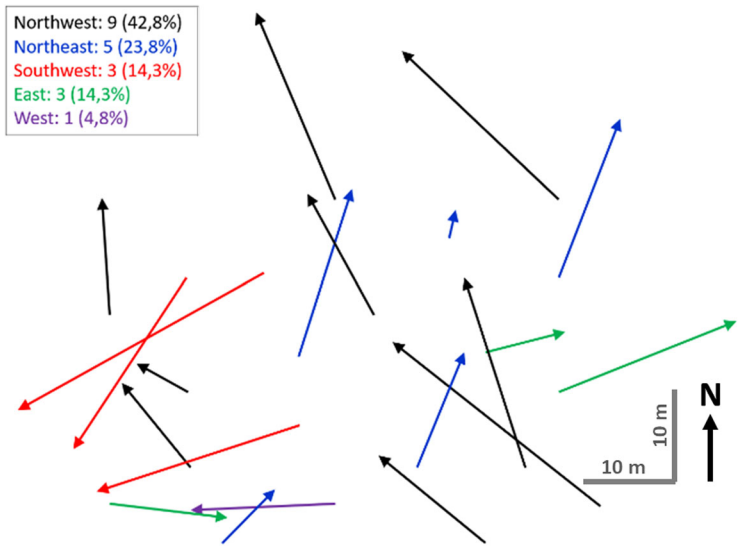

Fig. 8. Qualitative sketch of the overall direction of the deviation of the 21 randomly selected boreholes and length of the deviation. Based on measurements described in Nordell et al. (2016, fig. 11).

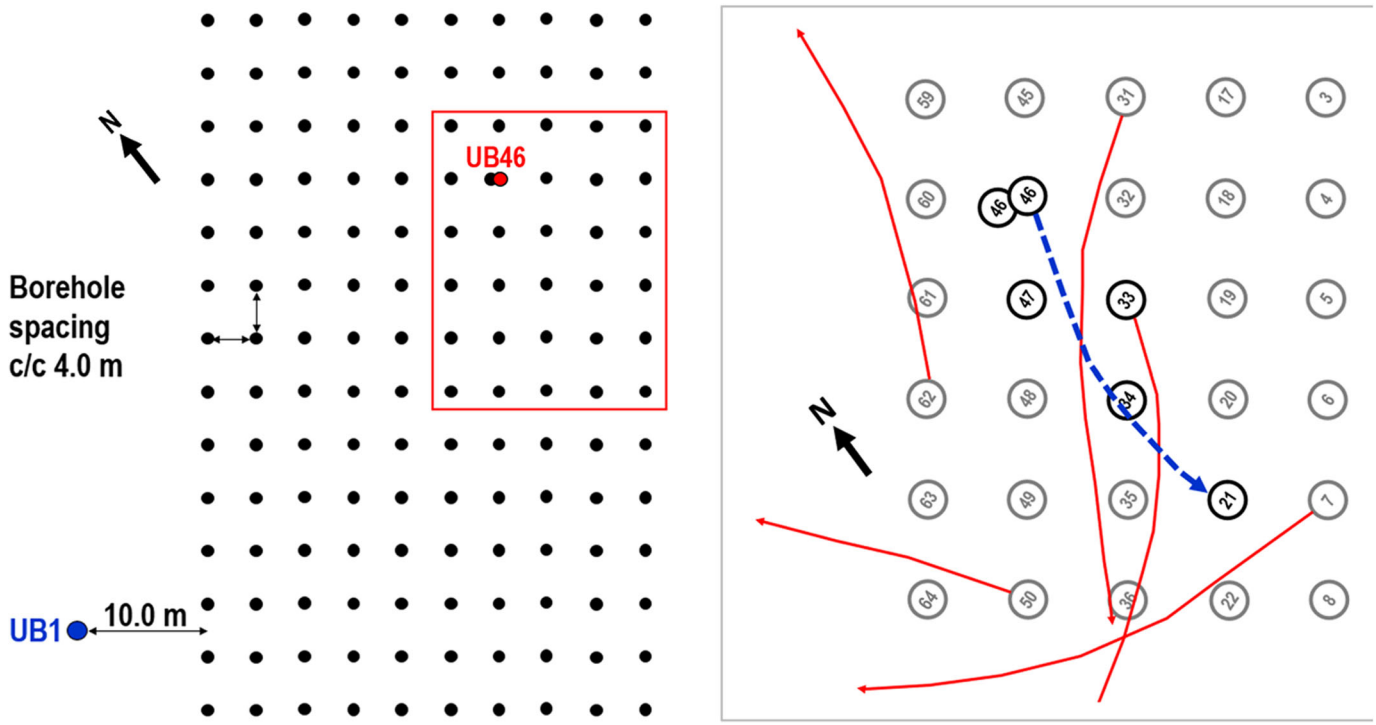

Fig. 9. A selected part of the BTES (to the right), described in Nordell et al. (2016), shows the assumed borehole deviation for UB46 (blue dotted line), which was terminated due to drilling into borehole 21. The sketch shows that the borehole is near borehole 34, and near borehole 21 near the bottom. The measured borehole deviation for some of the other boreholes (red lines) shows that the paths of boreholes 31 and 33 can be near observation borehole UB46.

From November 15, 2018, to February 7, 2019, there was a continuous heat extraction from the BTES.

The mean undisturbed ground temperature was measured as around 8 °C in the two old test boreholes (200 m) on the other side of the dam (Andersson 2011).

UB1 is placed 10 m away from the BTES. The temperature profile in UB1 has a linear pattern from about 25 to 130 m, increasing from ~22 to 30 °C. This temperature is the result of 9 years of conductive heat transfer (thermal charging since 2010). The temperature drops toward the surface and at the bottom toward the undisturbed ground temperature, as expected. The section with the linear gradient indicates that the heating mechanism is conduction. The linear temperature profile in UB1 indicates no neighboring/

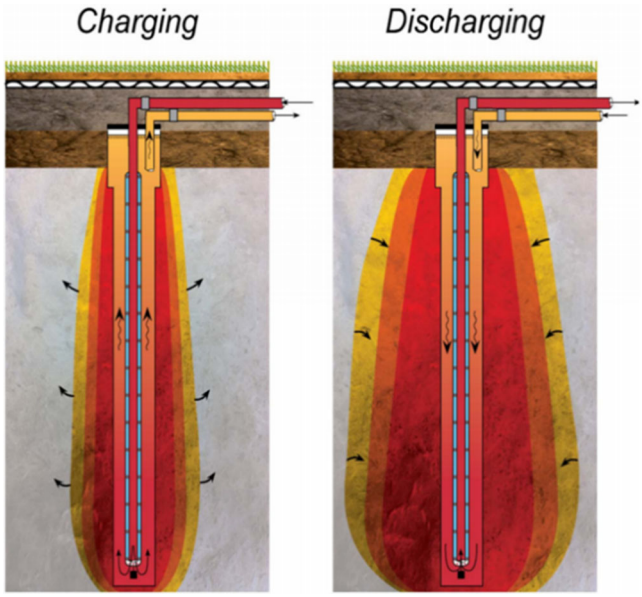

Fig. 10. The fluid flow of water in the open coaxial collector at Emmaboda is switched depending on heat charging or heat extraction (discharging) mode.

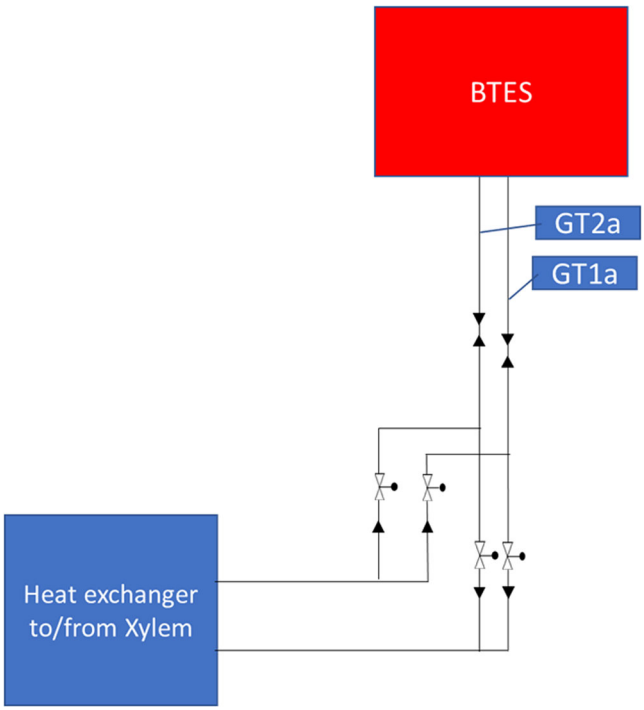

Fig. 11. Principle of temperature measurements in/out of the BTES. Owing to the change in flow directions during heat charging and heat extraction, GT1a and GT2a represent supply and return temperatures, depending on the heat charging/heat extraction state.

contact points with production boreholes disturbing this UB1. Even though there is a significant water-bearing fracture zone in the upper part of UB1 (Figure 7), there is no sign of groundwater flow in this section. This was expected due to the flat terrain and several open rivers and dams in the area (Figure 1), that is, no hydraulic gradient or inclination on the groundwater table. The consequence of groundwater flow would have been an extra heat transport by convection, as illustrated on a principal basis in Figure 14.

Groundwater flow in the water-bearing fractures due to a hydraulic gradient would have been visible as a section in the borehole with lower/higher temperatures caused by groundwater flow with lower/higher temperatures. The feasibility of a BTES in crystalline bedrock with fracture permeability depends on the hydrogeological conditions. In a normal situation, which is also the case at Emmaboda, the crystalline bedrock consists of several fracture systems filled with groundwater. Still, the hydraulic conditions of the fracture systems imply no or minimal groundwater flow, probably due to the hydraulic connection to the nearby dam with a steady water table all over the year, that is, no hydraulic gradient. A hydraulic gradient greater than 0 is a prerequisite for a regional groundwater flow. The results from three thermal response tests preliminary to the construction of the BTES support the findings of no or negligible groundwater flow. The measured in situ effective thermal conductivity average was 3.0 W/m·K and corresponds with laboratory measurements of a similar rock type ("granite, granodiorites") with the same mineralogic composition that have a median value of 3.0 W/m·K (Ramstad et al. 2014). Similar effective thermal conductivities in situ and in the laboratory, based on the mineralogical composition of the rock, indicate a conductive heat transfer only. Note that in situ values are approximately 10% higher than laboratory values (Liebel 2012; Midttømme et al. 2000). If the BTES area at Emmaboda had been affected by a regional groundwater flow, a higher effective thermal conductivity should have been measured in the thermal response tests due to the addition of the convective heat transfer contribution of the groundwater flow. However, further investigation of an eventual influence by a regional groundwater flow in the crystalline and fractured bedrock at Emmaboda is recommended. This should be done in a model study where the fluid flow is in fractures only, that is, with negligible porosity and permeability of the rock matrix. This was not a part of this study, but will give a deeper understanding and wholeness of the hydrogeological and thermal interaction for the BTES in operation. Data can be made available through a request for further studies.

Since there is no sign of groundwater flow in UB1, the irregularities observed in UB46 might be explained by borehole deviation and interferences with other boreholes (Figures 8 and 9).

According to the temperature evolution following the heat extraction and charging temperatures of the neighboring boreholes, UB46 must pass quite near some other production boreholes along its path (Figure 9). UB46's temperature profile is approximately parallel to the profile in UB1 from ~30 to 60 m depth, increasing its temperature from about 32 to 35.5 °C. The most marked irregularity can be seen at about 80 m in depth, where the temperature is around 30 °C and significantly lower than the rest of the borehole. The

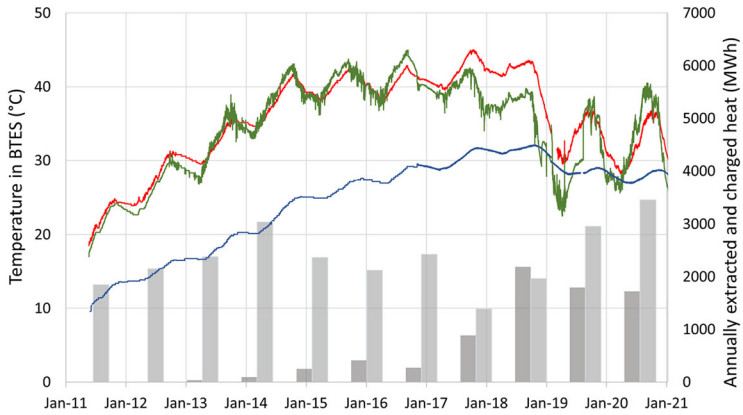

Fig. 12. Temperature development in UB1 (at 100 m) and UB46 (at 70 m and 117 m) in 2011–2021 during heat extraction and charging (annual values).

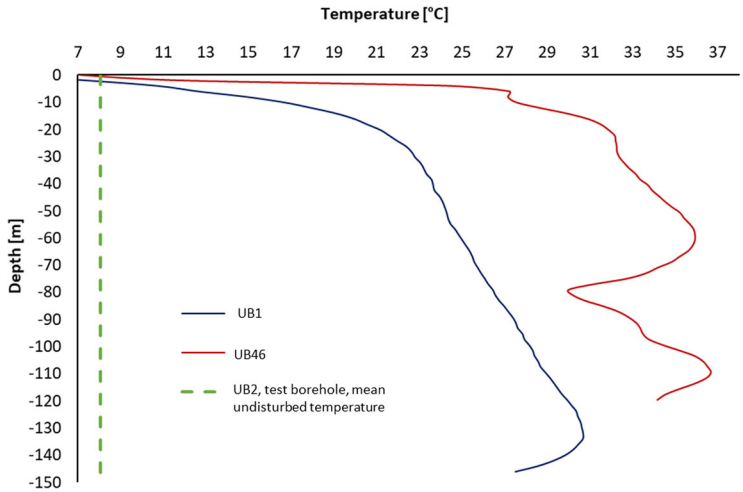

Fig. 13. Temperature profiles by DTS at Emmaboda on the of February 7, 2019, for the observation borehole UB1 outside the storage and observation borehole UB46 inside the storage. The mean undisturbed temperature in UB2 in the upper right corner of the borehole field is presented for comparison.

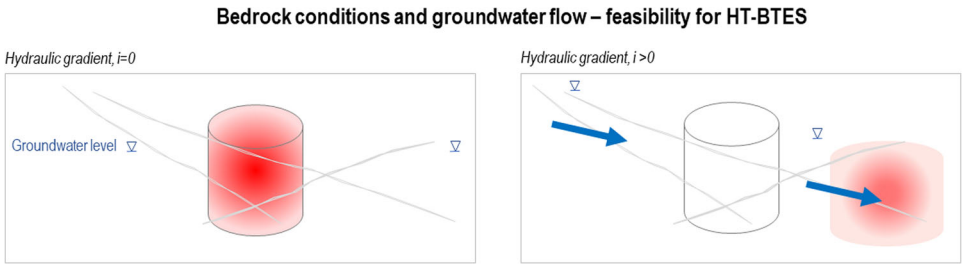

Fig. 14. Feasibility for an HT-BTES in crystalline bedrock concerning the risk of heat leakage by groundwater flow. The presence of water-bearing fractures (fracture permeability) in the bedrock and a hydraulic gradient ($i > 0$) in the area is a prerequisite for regional groundwater flow.

author's interpretation of this temperature variation is that UB46 has a contact point with or is very close to production borehole 34, as seen in Figure 9. When the measurement was performed, borehole 34 had been in extraction mode (coldest water in the annulus, see Figure 10) for almost 3 months, and the temperature is significantly lower than the temperature in the storage volume at the same depth. An irregular pattern for UB46 can also be seen at approximately 10 m and from 80 to 120 m depth. The maximum temperature along this profile is 36 °C at about 110 m. An interpretation is that this temperature irregularity is influenced by the deviated pattern of production borehole 33. The temperature irregularity at 10 m can be related to production borehole 46. UB46 was drilled into borehole 21; thus, the temperature

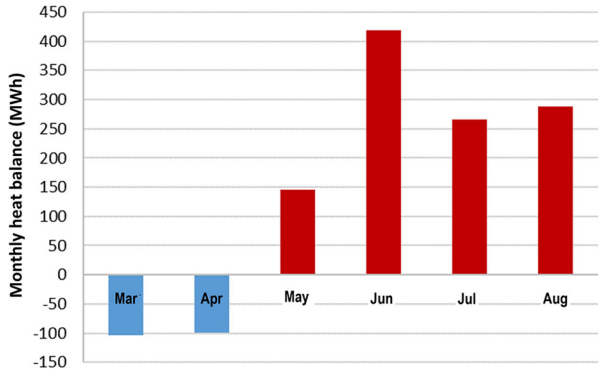

Fig. 15. Net heat extraction and charging from/to the BTES per month from March to August 2019. There is a net heat extraction from the f March 19 to April 30 and a net heat charging from May to August.

drop at 120 m is probably related to borehole 21, which has been in production, similarly to borehole 34, already described. Due to a deeper position and the coaxial flow direction during heat extraction, the temperature is higher at 120 m (production borehole 21) than at 80 m (production borehole 34). In theory, the temperature irregularities can also express different effective thermal conductivity values along UB46. However, the irregularities vary in magnitude with time and operation mode. The borehole path and distance to neighboring production boreholes seem to be the most probable explanation.

Temperature response in the storage (UB46) to heat extraction and charging

The specific heat extraction and charging per borehole are unknown, and each borehole is affected by its specific location.

Limitations of this section are:

- The temperature measurements are done in observation borehole UB46, that is, not in a production borehole. UB1 is 10 m away from the BTES; thus, it was not exploited for temperature measurements in the BTES.
- Heat extraction and charging refer to the total heat extracted and charged from/to the BTES. There are no energy measurements at the borehole level.

Figure 15 shows the net extraction and charging from/to the BTES from March 19 to August 31. There is a monthly net heat charging of the BTES by about 1100 MWh in this period. After the heat pump was installed in 2018, the accumulated heat extraction increased drastically, reducing the BTES temperature to approximately 25 °C in 2021. Figure 15 is presented here to ease the analysis of the temperature variations when the DTS was collecting data, but it does not represent the balance of 2019. Further information about energy balance and system performance can be found in Andersson, Rydell, and Håkansson (2021b).

Figure 16 shows selected temperature profiles in observation borehole UB46. All profiles are measured on the 19th of each month from March to August at 1700 hours. The profiles from March and April with energy extraction are shown to the left, while the temperature profiles measured during the heat charging period of the BTES in May, June, July, and August can be seen to the right. Note that there is heat extraction and heat charging in May 2019. The temperature anomaly around 80 m depth is visible in both operation modes. The temperature anomalies at around 10, 35 to 40, and 100 m depth are clearer in charging mode. The differences observed in the measured temperatures between 80 and 100 m can be explained by the differences in flow resistance related to the heat carrier flow with neighboring boreholes and thermal interaction with neighboring production boreholes. More details are given in connection to Figure 13, and to a possible observation of thermosiphon discussed in the transient temperature section given later.

Energy analysis of heat extraction and charging versus temperature development in UB46

Figure 17 shows the temperature evolution throughout the measuring period at some selected borehole depths (10, 35, 60, 80, 83, 100, 110, and 120 m). These borehole depths mostly correspond with the irregularities in the temperature profile in UB46 with heat extraction and injection. The temperatures at some levels (60, 110, and 120 m) follow the same pattern, with minor variation from ~32 to 35 °C. The lowest temperature can be seen around May 20, when the mode switches from heat extraction to charging. The temperatures at 80 and 83 m fluctuate the most, followed by the temperature variations at 100 m depth. The temperature at 10 m depth has the most significant temperature variation, possibly due to two main reasons: (1) a lower thermal conductivity of the upper soil layer as compared to the bedrock (slower temperature response) and (2) the temperature of the circulating fluid, which is lowest/highest at the top of the storage during extraction/charging periods.

The temperature sensors GT1a and GT2a (Figure 17) are in the technical room. In heat charging mode, the sensor GT1a shows the temperature entering the boreholes and GT2a the return temperature from the boreholes. In heat extraction mode, the flow direction is switched, and then GT1a shows the return temperature and GT2a the supply temperature to the boreholes (see Figure 11 for an illustration of the connection). The periods when the GT1a and GT2a temperatures are lower than the temperatures in UB46 imply heat extraction from the BTES, and vice versa, that is, heat charging when GT1a and GT2a temperatures are higher than the temperatures in UB46. The range of heat charging temperatures varies between 60 and 30 °C, with a maximum temperature difference to the return temperature of 23 °C. The average ΔT is around 10 K.

Figure 18A–C shows the temperature evolution at selected depths and the corresponding heat exchange in the BTES during some chosen periods during 2019: (A) heat extraction only (8 days), (B) both heat extraction and charging from/to the BTES (7 days), and (C) heat charging only (6 days).

Period (A)—Heat extraction (Figure 18A). The heat extraction from the storage is nearly constant, providing a

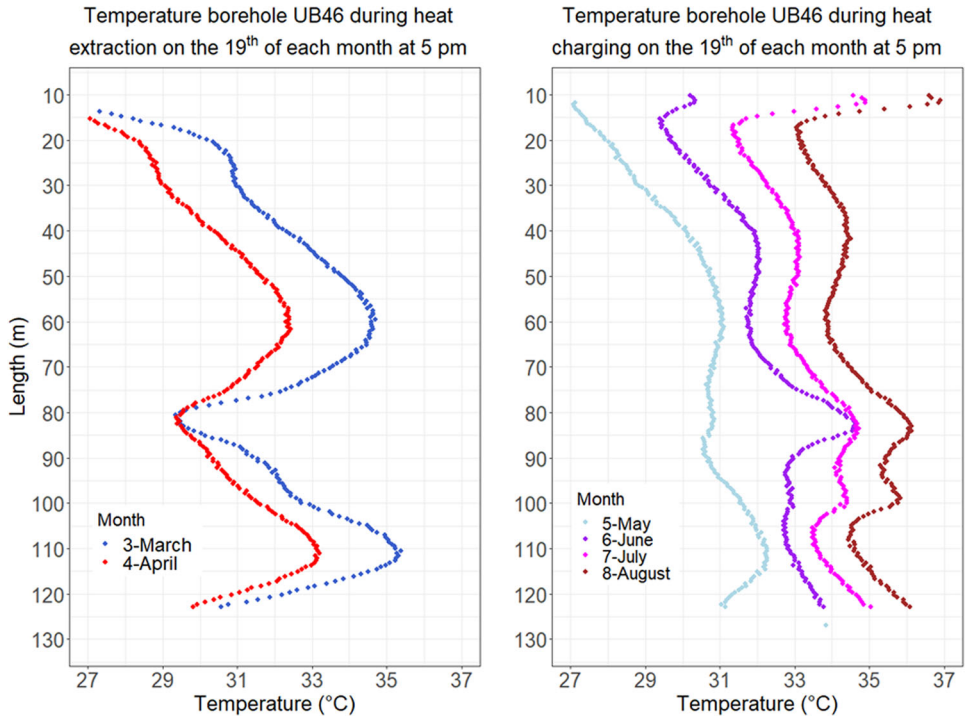

Fig. 16. Temperature profiles in observation borehole UB46 during heat extraction (to the left) in March and April and heat charging (to the right) in May, June, July, and August. Note that there is both heat extraction and heat charging in May 2019.

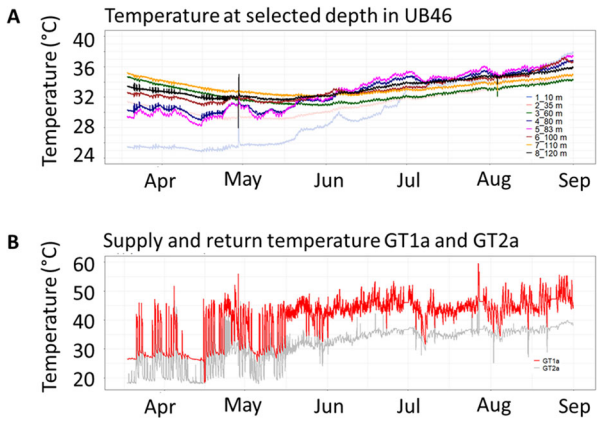

Fig. 17. (A) Temperature evolution in UB46 throughout the measuring period for selected depths (10, 35, 60, 80, 83, 100, 110, and 120 m) during heat extraction and charging in 2019. (B) The GT1a- and GT2a-temperature sensors in the manifold control the temperature from and to the BTES, respectively.

steady decrease in temperature of around 1 degree at 60, 100, 110, and 120 m depth during the seven days. The temperature decrease at 80-83 m depth responds more quickly to the heat extraction and is around 2 to 5 degrees lower than the rest during the seven days. The net heat extraction from the BTES during this period is 88,324 kWh. Assuming an even extraction per borehole for the seven days (168 h), around 3.75 kWh/h is extracted per borehole, or a specific extraction of at least 25 W/m, considering the number of boreholes in operation and the operation hours per borehole section. A specific heat extraction of 25 W/m is normal for a standard ground source heat system in Norway and Sweden with a standard single U-collector (Holmberg et al. 2016). The maximum measured heat extraction is around 700 kWh/h, which is assumed to be evenly distributed among the boreholes ($140 \times 150 = 21\ 000$ m), giving a maximum specific heat extraction per borehole meter of 33 W/m.

Period (B)—Heat extraction and charging (Figure 18B). The temperature response is more reactive during the period with heat extraction and charging. In periods with variations between heat extraction and heat charging, ripples are observed in the temperature evolution at 80 and 83 m in depth following the production borehole 34, as described in connection to Figure 13. The net heat balance in this period is 21,853 kWh. Some days the variation goes between about 1000 kWh/h of heat charging (at least 48 W/m) and 700 kWh/h (at least 33 W/m) in heat extraction, considering the number of boreholes in operation and the operation hours per borehole section.

Period (C)—Heat charging (Figure 18C). The temperature increase reflects the variation in the heat charging during the day, with the 83 m depth clearly showing the most significant response. The temperature increase varies between ~0.5 and 1.3° for all depths and the zone around 83 m, respectively. The net heat charging of the BTES in these specific eight days is 79,730 kWh (at least 19.8 W/m, considering the number of boreholes in operation and the operation hours per borehole section).

Transient temperature profiles in UB1 and UB46 from March to September

Figures 19 and 20 show the temperature profiles measured in UB46 and UB1 in the whole period from March 19 to

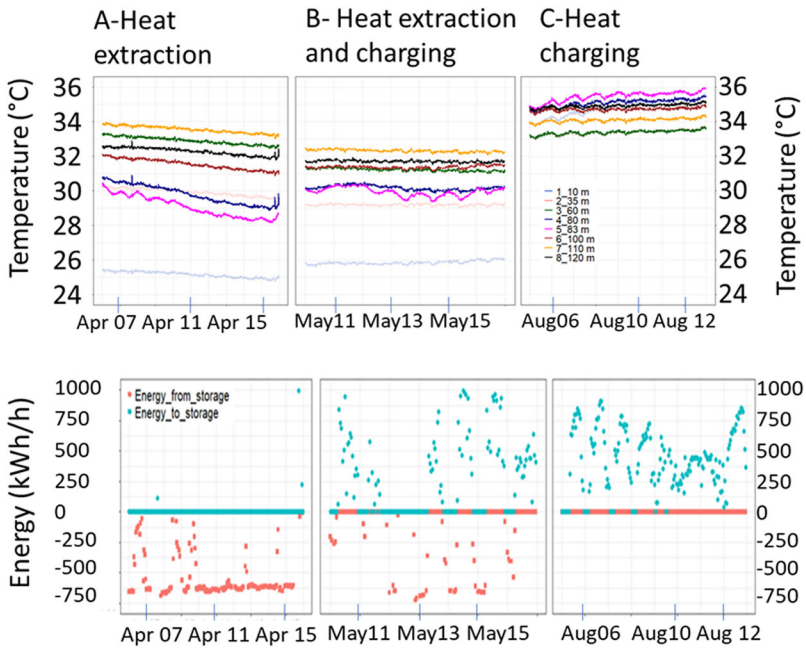

Fig. 18. Data from UB46 showing the temperature evolution at selected depths and the corresponding heat exchange in the BTES during some chosen periods of (A) heat extraction (8 days), (B) both heat extraction and charging from/to the BTES (7 days), and (C) heat charging only (6 days).

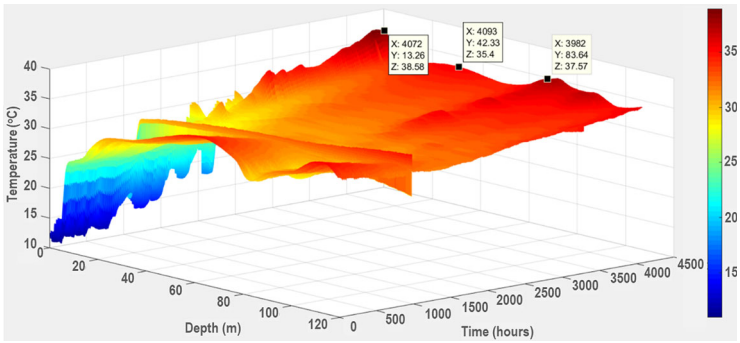

Fig. 19. Measured temperature profile in UB46 inside the storage from March 19 to September 5, 2019 (x-axis, hours). The temperature (z-axis) varies from around 15 °C at the top of the borehole to around 37–38 °C at 13 and 84 m depth (y-axis). A temperature peak can also be seen at around 42 m.

September 5, 2019. The storage is used for heat extraction until March 21, alternating heat extraction and charging from March 21 to May 30, and heat charging only from May 30 to August 30. Note that there have been some cold mornings with minor heat extraction during the period of heat charging, but these are considered outliers as the periods are short.

The shape of the temperature profiles in UB1 (Figure 20) remains almost unchanged during the entire period. However, careful observation of the temperature levels shows that the bottom part of the ground is successively heated up more than the top, while the upper part becomes colder. In the coaxial boreholes, the heat is injected through the inner pipe of the borehole heat exchangers; thus, most heat is injected at the bottom of the borehole, and the storage volume slowly increases the temperature upward.

As indicated earlier by the temperature profile measurement during the fiber installation day, February 7, the presence of groundwater flow could have explained one or several of the peaks in UB46 but is unlikely due to the entire conductive behavior in UB1 verified by, for example, the flat terrain and no hydraulic gradient, as well as measured effective thermal conductivity from the thermal response tests.

The temperature profile in UB46 varies according to the heat extraction and charging mode of the BTES. The temperature levels vary from around 15 °C at the top of the borehole to about 37–38 °C at 13 and 84 m depth, respectively. A softer temperature peak can also be seen around 42 m. The temperature variation at around 13 m represents the transition zone between the soil and the bedrock. The effect of the lower thermal conductivity of the soil compared to

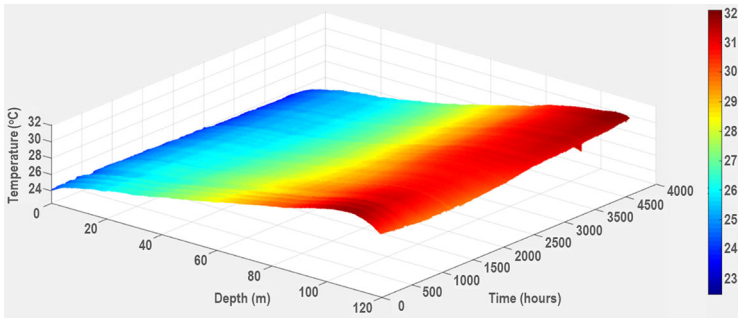

Fig. 20. Measured temperature profile in UB1 outside the storage from March 19 to September 5, 2019. Despite a large fracture zone in the borehole at 30 m depth, the thermal profiles show an entirely conductive response, and there is no groundwater flow through this borehole.

the higher thermal conductivity of the bedrock means that the soil gets colder during heat extraction from the storage, and vice versa, warmer during heat charging of the storage.

Some internal and local groundwater flow inside parts of UB46 cannot be excluded, for example, due to temperature differences (thermosiphon). However, the "wave pattern" of the temperature profiles in UB46 (Figure 16) indicates that hydraulically driven groundwater flow influence is unlikely. A possible hydraulically driven groundwater flow would have shown as sections with even temperatures, between fractures with inflowing and outflowing groundwater. An exception from this statement can occur between 80 and 100 m depth, which a thermosiphon effect might cause, especially in charging mode (Figure 16), where warm water is injected into the center of the coaxial collector and rises by the annulus (Figure 10). The temperature difference between the injected water in the production boreholes and the water in the observation borehole, for example, at 100 m, might be high enough to cause a thermosiphon effect with up-flowing warmer water that could justify the profile between 80 and 100 m in Figure 16. The lower heat flux in extraction mode compared to charging can explain why the temperature profiles in this section varies so distinctly.

The diagrams in Figure 18 demonstrate the inertia of the ground by temperature variations in observation borehole UB46 through periods of heat extraction and charging from/to the BTES. These are normal and agree with theory and how the storage is expected to perform at the temperature levels Emmaboda is operated with, similar to regular simulations and operation of other BTES systems.

Despite limitations in this dataset, the minor temperature changes during heat extraction and heat charging show, together with the temperature profiles (Figure 16) and temperature evolutions (Figures 17 and 18), that there is a potential for higher thermal power rates in both heat extraction and charging modes at Emmaboda.

The higher heat exchange capacity of the BTES system is possible for limited periods (hours). However, several other limiting factors must be considered, such as a maximum flow rate, the maximum vacuum pressure of the heat carrier loop, and the temperature limits for the system (which might be exceeded if higher power rates are used).

Conclusions

The first fiber optical temperature profile measurements in two observation boreholes at Emmaboda BTES in Sweden give valuable insights into heat transfer details inside and in the vicinity of the borehole thermal energy storage during the operation. The temperature profiles in groundwater-filled observation boreholes were measured in February and from March 19 to September 5, 2019. The fiber cable position in the borehole is random, for example, in the middle (groundwater) and close to the bedrock of the borehole wall. At one of the oldest and best documented BTES systems in operation, the DTS measurements in the two observation boreholes UB1 and UB46 at Emmaboda give a deeper understanding of the essential factors influencing the design, construction, and operation of BTES. The main findings from the study at Emmaboda are:

- Borehole deviation is the most complex factor in interpreting the temperature profile measurements and understanding the heat transfer results. The interpretation of the temperature profiles in UB46 at Emmaboda is an example of this. Here the information about the borehole deviation of 15% (21 out of the 140) of the boreholes (Nordell et al. 2016) had to be carefully examined to achieve a realistic interpretation of the observed temperature irregularities, which varied with depth and operation mode. The temperature profile deviates significantly from a theoretical conductive temperature profile. In new projects, the influence of the borehole deviation from the theoretical vertical position should get more attention and be further examined by 3D and four-dimensional (4D) modeling, design, documentation and visualization. This, together with continuous DTS monitoring of several production and observation boreholes for complete thermal control and following operation of new BTES systems, can enhance short- and long-term thermal performance.
- The unique coaxial collector used at Emmaboda with switching flow direction in heat extraction and charging mode affected the temperature results and had to be considered when analyzing the data.
- Based on the temperature profiles measured in the observation borehole UB46 inside the BTES, operation

mode, information of the borehole deviations, and neighboring boreholes, UB46 is interpreted to have contact points or be in the vicinity of production boreholes at the following depths:

- 10 m: borehole 46.
- 80 m (largest irregularity): borehole 34.
- 110 m: borehole 33.
- 120 m: borehole 21.

- The temperature response in UB46 seems more visible in heat charging mode than in heat extraction mode, maybe due to higher temperature levels during heat charging and subsequently higher heat flux.
- The temperature in UB46 varies by a few degrees throughout the measurement period, where the operation modes vary among heat extraction only, both heat extraction and heat charging, and heat charging only. The small temperature variation indicates that the storage operates appropriately and that large quantities of stored heat are available for extraction. The storage volume seems to have the capacity for higher heat extraction rates, but several other limiting factors must be considered (maximum flow capacity, maximum vacuum pressure of the heat carrier loop, and temperature limits for the system).
- The temperature profiles measured in observation borehole UB1, located 10 m outside the BTES, show an even and smooth gradient parallel to the geothermal gradient in the entire borehole during the measurement period. The measured in situ effective thermal conductivity in the preinvestigation phase correlates with the expected thermal conductivity value based on the mineralogical composition of the rock. If a regional groundwater flow had been present at Emmaboda, a significantly higher value (convective heat transfer contribution) of the effective thermal conductivity should have been measured in the thermal response tests. Even though there is a major water-filled fracture zone at approximately 30 m in depth, these results, in combination with the flat terrain and several open rivers and dams in the area, imply that there is no hydraulic gradient and verify that the measurement is not disturbed by a regional groundwater flow. No groundwater flow means that the heat loss of the BTES is conductive only.

In further work, it is recommended that observations investigate an eventual influence by a regional groundwater flow in the crystalline and fractured bedrock at Emmaboda. This should be done in a model study where the fluid flow is in fractures only, that is, with negligible porosity and permeability of the rock matrix. The model study will give a deeper understanding and wholeness for the hydrogeological and thermal interaction for the BTES in operation.

Nomenclature

BHE = borehole heat exchanger
BTES = borehole thermal energy storage
DTS = distributed temperature sensing
GT1a, GT2a = supply and return temperatures to/from the BTES
HT-BTES = high-temperature BTES
UB1 = observation borehole 10 m away from the BTES
UB46 = observation borehole in the BTES

Acknowledgments

This article was written within the research project (281000) "RockStore —develop, demonstrate and monitor the next generation BTES systems." The authors gratefully acknowledge the support from the Research Council of Norway (ENERGIX program) and the project partners. Additionally, Xylem Emmaboda has been responsible for obtaining the energy measurements, and the authors acknowledge their gratitude.

Conflicts of interest

The funders had no role in the design of the study, in the collection, analyses, or interpretation of data, in the writing of the article, or in the decision to publish the results. No potential conflict of interest was reported by the authors.

Funding

This work was supported by Norges Forskningsråd.

ORCID

Randi K. Ramstad http://orcid.org/0000-0001-9614-636X

References

Acuña, J. 2013. Distributed thermal response tests: New insights on U-pipe and Coaxial heat exchangers in groundwater-filled boreholes. Doctoral Thesis in Energy Technology at KTH in Stockholm, Sweden.

Andersson, O. 2011. TERMISK RESPONSTEST ITT Flygt, Emmaboda Undersökningsborrhål 2.

Andersson, O., L. Rydell, and N. Håkansson. 2021b. Case study report for the Xylem HT-BTES plant in Emmaboda, Sweden—Efficiency by using heat pumps for extraction of stored heat. In IEA HPT Annex 52—Long-term performance monitoring of GSHP systems for commercial, institutional and multifamily buildings. doi:10.23697/j2hk-4x61

Andersson, O., L. Rydell, and T. Algotsoon. 2009. Efficient usage of waste heat by applying a seasonal energy storage (BTES) at ITT Water & Wastewater AB, Emmaboda, Sweden. EffStock Conference in Stockholm.

Andersson, O., N. Håkansson, and L. Rydell. 2021a. Heat pumps rescued Xylem's heat storage facility in Emmaboda, Sweden. *The REHVA European HVAC Journal* 58 (4):23–7.

Bakker, M., Caljé, R. Schaars, F. Made, K.-J. van der Made, and S. d. Haas. 2015. An active heat tracer experiment to determine groundwater velocities using fiber optic cables installed with

direct push equipment. *Water Resources Research* 51 (4): 2760–72. doi:10.1002/2014WR016632

Bense, V. F., T. Read, O. Bour, T. Le Borgne, T. Coleman, S. Krause, A. Chalari, M. Mondanos, F. Ciocca, and J. S. Selker. 2016. Distributed temperature sensing as a downhole tool in hydrogeology. *Water Resources Research* 52:9259–73. doi:10.1002/2016WR018869

Brange, L., J. Englund, K. Sernhed, M. Thern, and P. Lauenburg. 2017. Bottlenecks in district heating systems and how to address them. *Energy Procedia* 116:249–59. doi:10.1016/j.egypro.2017.05.072

Ghafoori, Y., A. Vidmar, and A. Kryžanowski. 2022. A dynamic calibration of optical fiber DTS measurements using PEST and reference thermometers. *Sensors* 22 (10):3890. doi:10.3390/s22103890

Holmberg, H., J. Acuña, E. Naess, and O. K. Sønju. 2016. Thermal evaluation of coaxial deep borehole heat exchangers. *Renewable Energy* 97:65–76.

Jokiel, M., D. Rohde, H. Kauko, and H. T. Walnum. 2020. Integration of a high-temperature borehole thermal energy storage in a local heating grid for a neighborhood. International Conference Organised by IBPSA-Nordic, 13th–14th October 2020, OsloMet. BuildSIM-Nordic 2020.

Justo-Alonso, M., and J. Stene. 2013. State-of-the-art analysis of nearly zero energy buildings country report IEA HPP Annex 40 Task 1—NORWAY. (April).

Justo-Alonso, M., R. K. Ramstad, H. Holmberg, H. T. Walnum, K. Midttømme, and G. Andersen. 2020. Fjell 2020 high temperature borehole energy storage – system control for various operation modes. *WGC 2020*.

Kallesøe, A. J., and T. Vangkilde-Pedersen. 2019. HEATSTORE. Underground Thermal Energy Storage (UTES)—State-of-the-art, example cases and lessons learned. HEATSTORE project report, GEOTHERMICA - ERA NET Cofund Geothermal. 130 pp + appendices.

Klempa, M., Z. Rozehnal, M. Porzer, P. Bujok, D. Grycz, and A. Pytlyk. 2014. The construction of "Borehole Thermal Energy Storage" in miocene rocks on locality of Green Gas DPB, a.s. in Paskov (Czech Republic). International Multidisciplinary Scientific GeoConference Surveying Geology and Mining Ecology Management, SGEM, Albena, Bulgaria.

Kvalsvik, K. H., R. K. Ramstad, K. Midttømme, and H. Holmberg. 2022. Distributed temperature sensing measurements for exploring borehole thermal energy storages in Norway. European Geothermal Congress 2022 (EGC 2022), Berlin, Germany.

Lanahan, M., and P. Tabares-Velasco. 2017. Seasonal thermal-energy storage: A critical review on BTES systems, modeling, and system design for higher system efficiency. *Energies* 10 (6):743. doi:10.3390/en10060743

Liebel, H. T. 2012. *Influence of groundwater on measurements of thermal properties in fractured aquifers*. Thesis for the degree of Philosophiae Doctor, NTNU Trondheim, Norway.

Lowry, C. S., J. F. Walker, R. J. Hunt, and M. P. Anderson. 2007. Identifying spatial variability of groundwater discharge in a wetland stream using a distributed temperature sensor. *Water Resources Research* 43 (10):1–9. doi:10.1029/2007WR006145

Malmberg, M. 2017. *Transient modeling of a high temperature borehole thermal energy storage coupled with a combined heat and power plant*. Master of Science Thesis, KTH Stockholm, Sweden.

Malmberg, M., W. Mazzotti, J. Acuña, H. Lindståhl, and A. Lazzarotto. 2018. High temperature borehole thermal energy storage – A case study. In *IGSHPA Research Track*, 380–89. Stockholm Sweden. doi:10.22488/okstate.18.000036

Mesquita, L., D. McClenahan, J. Thornton, J. Carriere, and B. Wong. 2017. Drake landing solar community: 10 years of operation. IEA SHC International Conference on Solar Heating and Cooling for Buildings and Industry. ISES Solar World Congress.

Midttømme, K., B. O. Hilmo, H. Skarphagen, and A. Nissen. 2000. *Kartlegging av energipotensialet i berggrunnen på kartblad Bekkestua*. Baerum kommune: Varmeledningsevnen til bergarter.

Moldashi, D. N. 2021. Methods and technical solutions for keeping the path of a geotechnological borehole. *Mining Science and Technology (Russian Federation)* 6:42–51.

Monzo, P., A. Lazzarotto, and J. Acuna. 2017. First measurements of a monitoring project on a BTES system. IGSHPA Technical Conference and Expo Denver US March 14–16, 2017.

Morchio, S., and M. Fossa. 2020. On the ground thermal conductivity estimation with coaxial borehole heat exchangers according to different undisturbed ground temperature profiles. *Applied Thermal Engineering* 173:115198.

Morchio, S., M. Fossa, and R. A. Beier. 2022. Study on the best heat transfer rate in thermal response test experiments with coaxial and U-pipe borehole heat exchangers. *Applied Thermal Engineering*. 200:117621.

Murphey, C. E., and J. B. Cheatham. 1966. Hole deviation and drill string behavior. *Society of Petroleum Engineers Journal* 6 (1): 44–54.

Nilsson, E. 2020. Borehole thermal energy storage systems for storage of industrial excess heat: Performance evaluation and modelling. Licentiate thesis, Linköping University.

Nordell, B., O. Andersson, L. Rydell, and S. Liuzzo. 2014. Long-term performance of the HT-BTES in Emmaboda, Sweden. Greenstock 2015, International Conference on Thermal Energy Storage, Beijing, China. https://www.diva-portal.org/smash/get/diva2:1005848/FULLTEXT01.pdf. (DL 2018-05-07).

Nordell, B., S. Liuzzo, O. Andersson, L. Rydell, and B. Carlsson. 2016. Long term evaluation of operation and design of the Emmaboda BTES. Operation and experiences 2010-2015.

Nußbicker, J., D. Mangold, W. Heidemann, and H. Müller-Steinhagen. 2003. Solar assisted district heating system with duct heat store in Neckarsulm-Amorbach (Germany). ISES Conference 2003, Göteborg, Sweden.

Persson, U., B. Moller, and S. Werner. 2014. Heat roadmap Europe: Identifying strategic heat synergy regions. *Energy Policy* 74: 663–81. doi:10.1016/j.enpol.2014.07.015

Rad, F. M., A. S. Fung, and M. A. Rosen. 2017. An integrated model for designing a solar community heating system with borehole thermal storage. *Energy for Sustainable Development* 36:6–15.

Ramstad, R. K., H. Holmberg, L. Bugge, and M. H. Riise. 2017. Sluttrapport Fjell2020 konseptutredning miljøløsninger.

Ramstad, R. K., K. Midttømme, H. T. Liebel, B. S. Frengstad, and B. W. Wissing. 2014. Thermal conductivity map of the Oslo region based on thermal diffusivity measurements of rock core samples. *Bulletin of Engineering Geology and the Environment* 74:1275–86. doi:10.1007/s10064-014-0701-x.

Ramstad, R. K., O. Rådstoga, H. Holmberg, W. Mazzotti, and J. Acuña. 2020. The Asker 800 m energy wells in Norway with two types of coaxial collector – planning, installation and operation. Nordic geological winter meeting Oslo, Norway 9th of January.

Regander, C. 2019. Method development of high temperature storage (+100 °C) in sedimentary bedrock. Final report project 45993-1 Energimyndigheten, Sweden. 53 pages.

Reuss, M. 2021. 6 – The use of borehole thermal energy storage systems. In *Woodhead publishing series in energy*, ed. LFBT-A in TESS, Second E Cabeza, 139–71. Cambridge, United Kingdom: Woodhead Publishing.

Røgen, B., C. Ditlefsen, T. Vangkilde-Pedersen, L. H. Nielsen, and A. Mahler. 2015. Geothermal energy use, 2015 country update for Denmark. World Geothermal Congress 2015, Melbourne, Australia.

Rydell, L. 2019. Integration av kylvärmepumpar och borrhålslager i industrisystem. *Geoenergi 2019 Bergen*. http://cger.no/doc/pdf/presentationsGeoEnergi2019/5februar/04-Norge.pdf.

Schilperoort, B., M. Coenders-Gerrits, W. Luxemburg, C. J. Rodríguez, C. Cisneros Vaca, and H. Savenije. 2018. Technical note: Using

distributed temperature sensing for Bowen ratio evaporation measurements. *Hydrology and Earth System Sciences* 22 (1): 819–30. doi:10.5194/hess-22-819-2018

Schneider, B. 2013. *Storing solar energy in the ground*. Eggenstein-Leopoldshafen: FIZ Karlsruhe - Leibniz Institute for Information Infrastructure.

Sensornet. 2018. *Oryx DTS User manual v4*. London, United Kingdom: Sensornet, 101 pages.

Sevault, A., O. Stavset, and M. Bantle. 2017. Potential for steam regeneration in Norwegian industry. Within the framework of RCN-funded KPN-project HeatUp, project no. 502000960. SINTEF Energy Research, Report no. TR A7610, 40 pages.

Sibbitt, B., D. McClenahan, R. Djebbar, J. Thornton, B. Wong, J. Carriere, and J. Kokko. 2012. The performance of a high solar fraction seasonal storage district heating system – Five years of operation. *Energy Procedia* 30:856–65. doi:10.1016/j.egypro.2012.11.097

Skarphagen, H., D. Banks, B. S. Frengstad, and H. Gether. 2019. Design considerations for Borehole Thermal Energy Storage (BTES): A review with emphasis on convective heat transfer. *Geofluids* 2019:1–26. doi:10.1155/2019/4961781

Statens energimyndighet. 2020. *Energiläget 2020*.

Stokuca, M., and J. Acuña. 2019. Installation av DTS System in Xylem, Emmaboda.

Tjernstrom, J., M. Nygren, Å. Annsberg, J. Jansson, and J. Acuna. 2016. Technical introduction to Akademiska Hus BTES at Stockholm. *GSHP Convention.*

Winterscheida, C., J. O. Dalenbäcka, and S. Hollerb. 2017. Integration of solar thermal systems in existing district heating. *Energy* 137: 579–85.